

ICH 2019

International Conference on Humanities

**ELECTROSPUN POLY (IONIC LIQUID) MEMBRANE BASED
SOLAR CELL FOR SUSTAINABLE CLEAN ENERGY**

Mini Thomas (a), Sheeja Rajiv (b)*

*Corresponding author

(a) Department of Chemistry, Anna University, Chennai, India, anjanarosechf@gmail.com

(b) Department of Chemistry, Anna University, Chennai, India, sheeja@annauniv.edu

Abstract

The quest for sustainable and clean energy production has incentivized the development of solar cell technology. Dye-sensitized solar cells (DSSCs) have a significant influence on this revolution. Efficient and stable electrolyte systems are necessary for the outdoor application of DSSCs. An innovative polymeric ionic liquid (PIL), poly 3-decyl-vinyl imidazolium methyl methacrylate tetrafluoroborate was synthesized, characterized and blended with poly (ethylene oxide) (PEO). The polymer fibrous membranes have been fabricated by electrospinning technique, which were used as the electrolyte for DSSCs. Electrospun nanofibrous membrane possess high porosity and excellent specific surface area that can imbibe large amount of liquid electrolyte into its interconnected network structure. These membranes were studied by scanning electron microscopy (SEM), Fourier transform infrared spectroscopy (FT-IR), X-ray diffraction (XRD), differential scanning calorimetry (DSC) techniques and investigated their physical characteristics such as porosity, electron uptake and ionic conductivity. Photovoltaic and electrochemical effects have been examined. PEO/PIL membrane was compared with PEO for their efficiency. From the result, it was seen that PEO/PIL membrane exhibited superior power conversion efficiency (η), excellent ionic conductivity and better long term stability compared to cell with liquid electrolyte and PEO membrane. This novel PEO/PIL membrane based electrolyte in DSSC showed promising potential for the production of clean energy.

2357-1330 © 2020 Published by European Publisher.

Keywords: Clean energy, dye sensitized solar cell, poly (ionic liquid), electrolyte, electrospun membrane, poly (ethylene oxide).

1. Introduction

1.1. Solar energy

The yearly raise in global energy consumption will effect in increase of demands towards natural resources such as coal, petroleum and natural gas. These natural resources will take thousands of years to form and it cannot be replaced as fast as they are being consumed. These traditional fossil based fuel usages caused environmental problems such as carbon dioxide emission and irreversible climate changes (Luis et al., 2019). Among the energy sources existing, solar energy can fulfill the world's ever growing energy needs (Muthuraaman et al., 2017). Photovoltaic cells directly convert solar energy to electricity.

1.2. Dye-sensitized solar cell (DSSC)

Among the photovoltaic cells, dye-sensitized solar cell (DSSC) has received widespread attention owing to their advantages such as simple fabrication, ecofriendly nature and remarkable energy conversion, which mimics some of the key processes in the natural photosynthesis during the operation (Ishanie et al., 2014). In general, DSSCs are composed of three parts: TiO₂ photo anode, a counter electrode and an electrolyte.

1.3. Electrolyte

The electrolyte can be considered as central among the DSSC components, since it takes the main function as a medium for charge transport (Buraidah et al., 2017).

Basic requirements of the electrolytes used for DSSCs are:

- The electrolyte must transport the charge carriers between electrodes with high redox potential.
- The electrolyte must guarantee high ionic conductivity and make good contact with the electrodes.
- The electrolyte must contain very good long term stability.

Highly efficient DSSCs usually utilize liquid electrolyte, but liquid electrolytes are prone to leak and evaporate making them unstable for outdoor application. Thus, quasi-solid state (QSS) electrolytes have been favoured owing to their considerably excellent conductivity, strong interfacial contact and high penetrative ability into the semiconductor (Yi-Feng et al., 2016). Electrospun polymer nanofibrous membranes in the form of QSS electrolyte caught a lot of attention due to their high porosity and their capacity to entrap large amount of liquid electrolyte and possessed an extremely high specific surface area (Mini & Sheeja, 2019).

1.4. Poly (ionic liquid) (PIL)

Recently, imidazolium based poly (ionic liquid) (PIL) electrolytes in DSSCs have received a lot of attention; due to their ability to show multiple functions upon tuning their molecular structure and also provide excellent long-term stability and power conversion efficiency (Xiaojian et al., 2012). The non-volatile imidazolium cations stop the unfavorable recombination reactions by blocking the possible sites for electron leakage on the TiO₂ surface and thereby enhance the performance of DSSCs (Hao-Wei et al.,

2018). It also increases the ionic conductivity of polymer matrix through charge transport network formation via π - π stacking of imidazole segment (Silvia et al., 2017). The oxygen atom present in the methyl methacrylate (MM) forms a co-ordination bond with the Li atom and improves the ionic conductivity of the electrolyte. As the PIL could not be electrospun due to their lower molecular weight, the synthesized PIL was blended with a polymer possessing high molecular weight to obtain nanofibrous membrane. Poly (ethylene oxide) (PEO) was selected as the blending polymer due to its high chemical stability and better ion transport due to the consolidation of their cation-complexation capability (Yanyan et al., 2015; Zebardastan et al., 2017). Blending with PIL can solve the problem of PEO crystallization that occurs below 60°C.

2. Problem Statement

Leakage and solvent evaporation of the liquid electrolyte diminishes the stability and efficiency of DSSCs, thus making them unfit for outdoor applications (Yi-Feng et al., 2016). The use of solid state material based electrolyte shows better stability and low efficiency due to their poor interfacial contact between the electrodes (Shanmuganathan et al., 2016). In recent years, many attempts have been made to improve performance of DSSCs by using electrospun based quasi-solid electrolytes. Authors have fabricated PIL based electrospun membrane (Hao-Wei et al., 2018) which exhibited power conversion efficiency of 9.26% and provided long term stability (i.e. 97% of initial cell efficiency) compared with the liquid electrolyte. The decreased cell efficiency for the cell with the liquid electrolyte was related to the predictable leakage of the liquid electrolyte and evaporation of the volatile organic solvent.

3. Research Questions

- How quasi-solid state electrolyte aid in enhancing the stability and efficiency of DSSCs?
- What is the significance of electrospun nanofibrous membrane morphology in the stability of DSSCs?
- Does the poly (ionic liquid) architecture affect the efficiency and stability of DSSCs?

4. Purpose of the Study

- To synthesise poly (ionic liquid) (PIL) viz., 3-decyl-vinyl imidazolium methyl methacrylate tetrafluoroborate through free radical polymerization to increase the efficiency of DSSCs.
 - To incorporate the prepared PIL into poly (ethylene oxide) and fabricate them into nanofibrous membrane via electrospinning technique for the higher uptake of liquid electrolyte.
 - To study the physical and electrochemical characterizations of the prepared membranes.
 - To fabricate DSSCs with electrospun membranes and their photovoltaic performances and stability are to be studied and compared with the liquid electrolyte containing DSSCs.

5. Research Methods

5.1. Materials

Poly (ethylene oxide) (PEO) (average $M_w = 200,000$ g/mol), iodine (I_2), lithium iodide (LiI), 4-tert-butylpyridine (TBP), Chloroform, Vinyl imidazole, Sodium tetrafluoroborate, Azobisisobutyronitrile (AIBN) and absolute ethanol were purchased from Sigma-Aldrich Co., Ltd. Methyl methacrylate and dichloromethane (DCM) were purchased from SRL Chemicals Pvt. Ltd., India. Nanocrystalline TiO_2 (nc- TiO_2) paste coated on FTO conducting glass ($15\Omega/sq$), cis-Diisothiocyanato-bis (2,20-bypyridyl-4,40-dicarboxylato) ruthenium(II) bis (tetrabutylammonium) (N719 dye) and Pt counter electrode were purchased from Greatcell Solar's DSL, Australia.

5.2. Preparation of electrospun polymer nanofibers

PEO solution (A) with a concentration of 11 w/v % was prepared in chloroform at room temperature. Solution (B) was prepared by adding 0.55 g of PIL in solution (A). The prepared polymer solution was loaded into a 5 mL syringe attached to a stainless steel needle with a diameter of 0.3 mm. The flow rate of the solution was adjusted to 3 mL/h with the help of a syringe pump. An aluminum foil was placed as a collector at a distance of 15 cm from the needle and a high voltage of 30 kV was applied at the end of the needle. The electrospinning parameters were set after optimization.

5.3. Fabrication of DSSC devices

The TiO_2 photo electrode was fabricated by immersing the annealed screen printed nc- TiO_2 into 0.5mM of N719 dye in absolute ethanol for 24 h at room temperature under dark conditions followed by rinsing with anhydrous ethanol and air dried. A gasket frame (MSOO4610-10) with an optimal thickness of 60 μm was inserted between the dye-adsorbed nc- TiO_2 electrode and Pt counter electrode and the cell was pressed together using clips. The gasket thickness was sufficient to allow for the addition of a sufficient amount of electrolyte. Quasi-solid state DSSCs was assembled using electrospun nanofibrous membrane of definite dimension being sandwiched between the dye imbibed TiO_2 working electrode and the Pt counter electrode (Marwa et al., 2016; Tan et al., 2019) and clipped tightly. A drop of the prepared electrolyte solution containing 0.05 M iodine, 0.1 M lithium iodide, 0.6 M of PMII, and 0.5 M of TBP in 1 mL of a mixture of valeronitrile (15%) and acetonitrile (85%) were then introduced into the clamped electrodes. The active area of the DSSC was found to be 0.49 cm^2 . For comparative studies, another DSSC was fabricated using liquid electrolyte without electrospun nanofibers.

6. Findings

6.1. Synthesis of poly (ionic liquid)

Poly (ionic liquid) (PIL), 3-decyl-vinyl imidazolium methyl methacrylate tetrafluoroborate was synthesized via a simple procedure, as shown in Figure 01. The ionic liquid (3-decyl-vinyl imidazolium bromide) was prepared by taking 1-vinyl imidazole (5 mL), 1-bromodecane (5 mL) in a round bottomed flask and immersed in an oil bath for 2 h at 100°C. It was cooled for 15 min and again heated for 25 min in

an oil bath to extract the ionic liquid by adding the solvent dichloromethane (Deyab et al., 2017). An aqueous solution of NaBF_4 (2 g) was then added and the solution was stirred continuously until phase separation occurred. The compound obtained was purified and dried in vacuum. The poly (ionic liquid) was prepared by free radical polymerization process. The monomers 3-decyl-vinyl imidazolium bromide and methyl methacrylate was taken and AIBN were used as an initiator. These three solutions were mixed well and kept in an oil bath under N_2 atmosphere and refluxed for 5 h. After 5 h, the polymer was precipitated out using water and evaporated in vacuum and the product poly (3-decyl-vinyl imidazolium methyl methacrylate tetrafluoroborate) was obtained as a pale yellow solid. The structure of the product was confirmed by ^1H NMR studies as follows: ^1H NMR (500 MHz) and solvent used was CDCl_3 ; 0.83 (3H, - CH_3 , t), 1.03-1.92 (2H, - CH_2 , m), 7.40 (1H, -CH, d), 7.59 (1H, -CH, d), 8.01 (1H, -CH, d), 0.96 (3H, - CH_3 , t), 1.77(2H, - CH_2 , m), 2.45(1H, -CH, s), 2.59(2H, - CH_2 , m), 1.96 (3H, - CH_3 , s), 4.10(3H, - CH_3 , s), 3.68 (3H, - CH_3 , s).

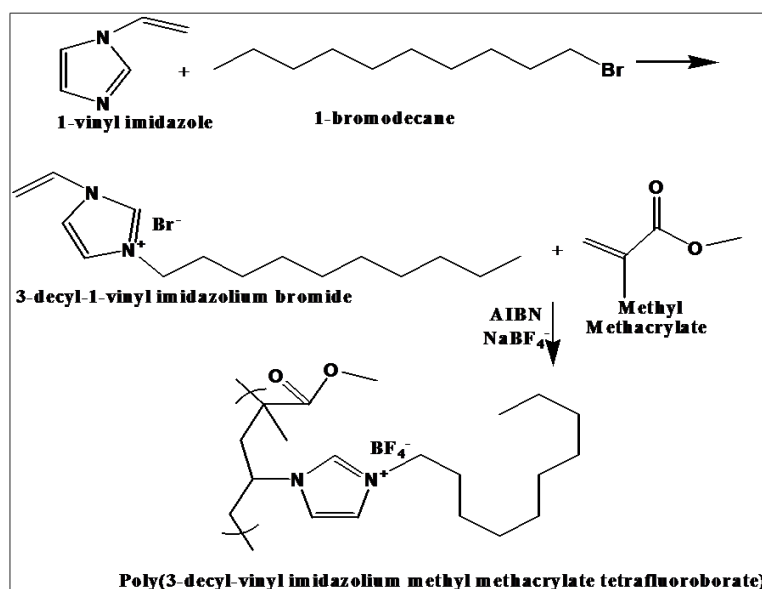


Figure 01. Preparation of poly (3-decyl-vinyl imidazolium methyl methacrylate tetrafluoroborate)

6.2. Study of the morphology

Figure 02 (A1) exhibited uniform; beadless, smooth pure PEO nanofibers with mean diameter of 181.3 nm as shown in Figure 02 (A2). The highly porous interconnected nanofibrous membrane imbibed large amount of liquid electrolyte into the pores. Figure 02 (B2) shows the SEM micrograph of PIL/PEO membrane which showed an increased fiber diameter and rougher fiber surface. Increased fiber diameter of 191.12 nm could be attributed to the increased viscosity of the solution upon the addition of PIL and rougher fiber surface may be due to the change in surface tension of the precursor solution (Chang et al., 2018). The rougher fiber surface increased the surface area thereby enabling higher uptake of electrolyte. The EDX spectrum in Figure 02 (B1) shows the presence of oxygen, nitrogen and boron apart from carbon. These results confirm the presence of imidazolium IL and methyl methacrylate. The presence of boron indicates the presence of boron trifluoride on the nanofibers.

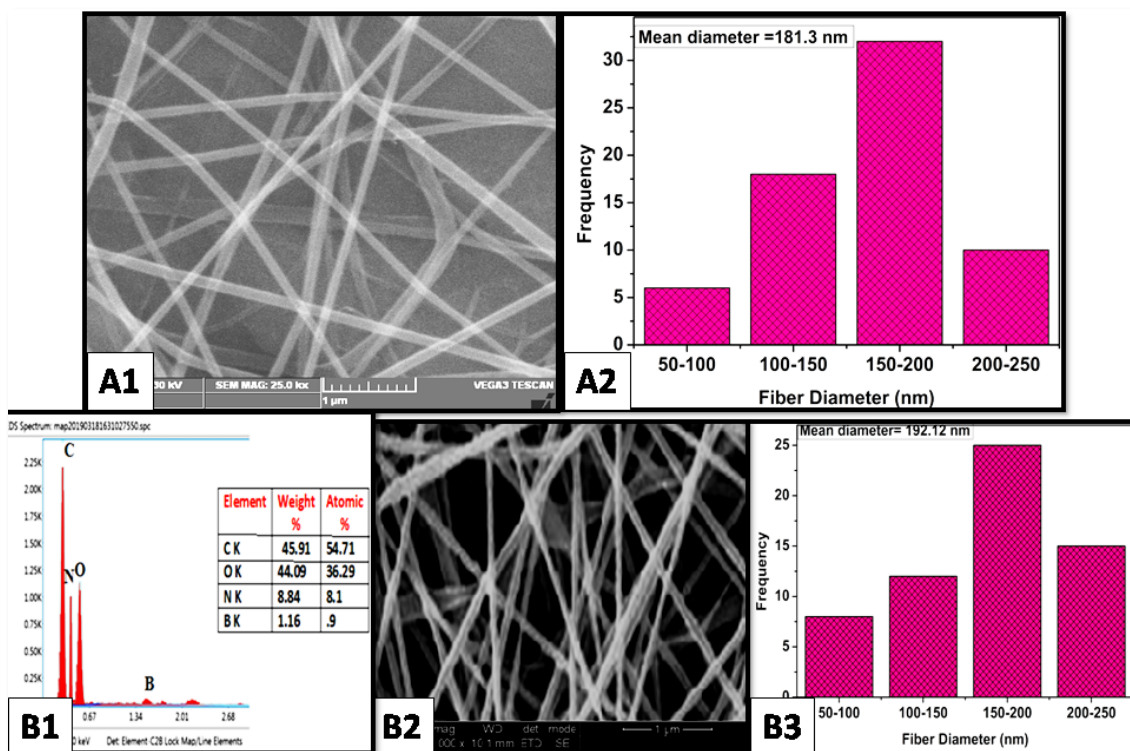


Figure 02. (A1) SEM images of electrospun PEO nanofibers (A2) Histogram of PEO nanofibers (B1) EDX spectrum of PIL/PEO membrane (B2) SEM image of PIL/PEO (B3) Histogram plot of PIL/PEO membrane

6.3. FTIR study

Figure 03 displays the FTIR spectra of synthesized poly (3-decyl-vinyl imidazolium methyl methacrylate tetrafluoroborate) (PIL), PEO nanofibers, PIL/PEO nanofibrous membrane in the 500-4000 cm^{-1} wave number range. In Figure 03 (A), the peak at 1250 cm^{-1} shows the C-N stretching. The peak at 1160 cm^{-1} indicates the presence of ester C-O-C stretching vibration. The band appearing at 1640 cm^{-1} displayed C=C stretching vibration.

The peaks at 2850 cm^{-1} and 1390 cm^{-1} indicate the presence of C-H stretching and C-H bending vibrations respectively. The FT-IR spectrum of PEO nanofibers in Figure 03 (B) showed an intense peak at 2892 cm^{-1} due to -CH₂ asymmetric stretching and at 839 cm^{-1} due to -CH₂ asymmetric bending vibrations respectively. The peaks at 1478 cm^{-1} and 1278 cm^{-1} represent the -CH₂ scissoring and -CH₂ symmetric twisting vibrations respectively. The band at 1097 cm^{-1} shows the presence of symmetric and asymmetric -C-O-C- stretching vibrations (Elashmawi & Gaabour, 2015). In the case of PIL/PEO nanofibers shown in Figure 03 (C), the peak nearer to 3000 cm^{-1} shows the asymmetric C-H stretching of -CH₂ and at 1700 cm^{-1} shows the C=O stretching vibration. The peaks at 1250 cm^{-1} shows the C-N stretching and the peak at 2000 cm^{-1} shows the C=N stretching vibration. All the functional groups of PEO and PIL were present in the blended fibers which revealed the interaction between PEO and PIL.

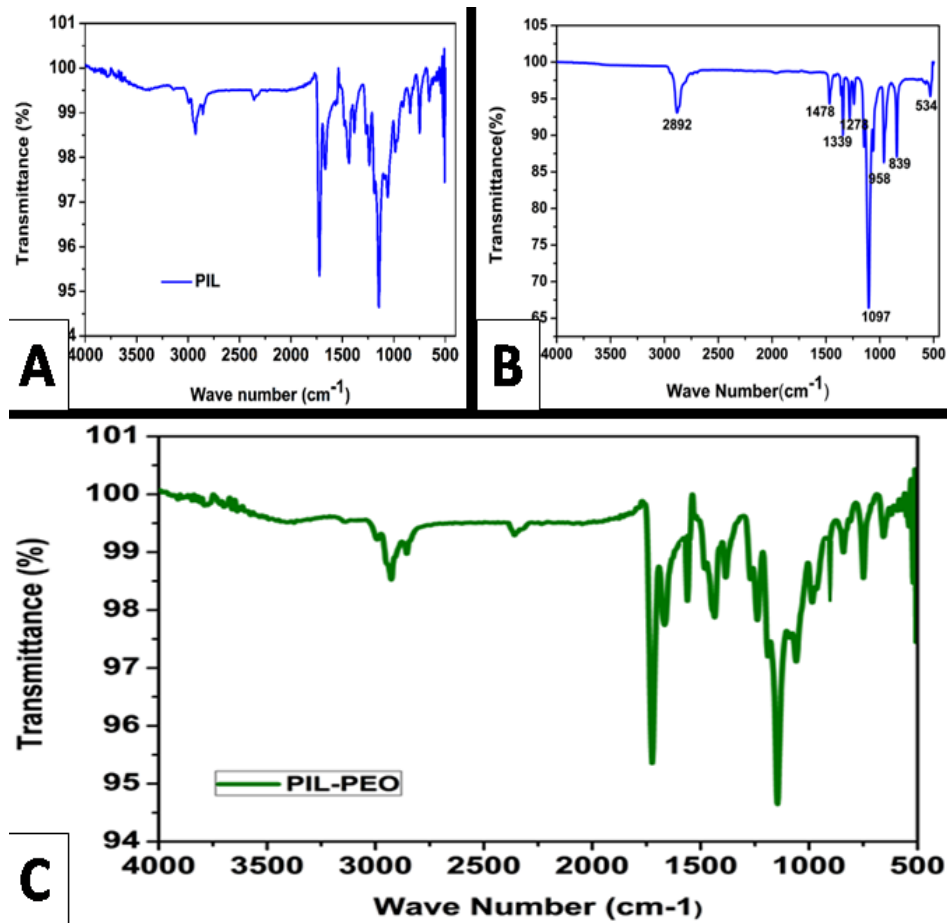


Figure 03. ATR-FTIR spectrum of (A) PIL (B) PEO nanofibers (C) PIL/PEO nanofibrous membrane

6.4. XRD analysis

Figure 04 shows the XRD pattern of PEO nanofibers and PIL/PEO blended nanofibers. The maximum intensity peaks were observed at 19.28° and 23.6° respectively for the PEO nanofibrous membrane. The sharp peaks indicate the crystalline nature of PEO, which originate from the ordering of PEO side chains due to strong intermolecular hydrogen bonding. In the case of PIL/PEO blend nanofibrous membrane, the crystalline peaks of PEO were not observed and an amorphous phase was dominant. The reason could be due to the disruption of the rigid bonding in PEO due to the addition of PIL which enabled the ion migration (Azli et al., 2015). The relative percentage of crystallinity ($X_c\%$) was calculated by using following equation (1) where, A_c is the crystalline area and A_a is the amorphous area and summarized in Table 1.

$$X_c \% = [A_c / (A_c + A_a)] \times 100 \quad (1)$$

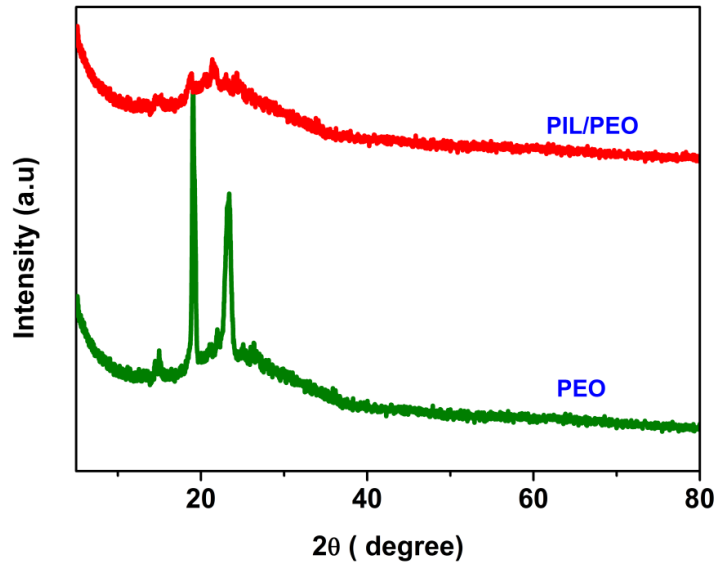


Figure 04. XRD spectra of PEO nanofibers and PIL/PEO nanofibers

6.5. Differential scanning calorimetric studies

Figure 05 shows the DSC thermograms of PEO nanofibers, PIL and PIL/PEO nanofibers in the temperature range of -70°C to 200°C . The melting peaks of PEO appeared at 64.55°C . The addition of PIL into PEO broadened the melting peak of PEO and the melting enthalpy decreased from 142 J/g to 137.12 J/g . This suggests that there was a reduction in the crystallization of PEO and thereby an enhancement in amorphous phase occurred which facilitated an increase in ionic conductivity. DSC thermogram of PIL showed an endothermic broad peak at 150°C due to the melting of PIL. In the case of PIL/PEO nanofibrous membranes, two endothermic peaks at 65°C and 150°C were observed corresponding to the melting of PEO and PIL respectively. Although the result showed the immiscibility of the polymer blend solution, the enhancement of ionic conductivity in the blended solution was found to be beneficial for the DSSC application.

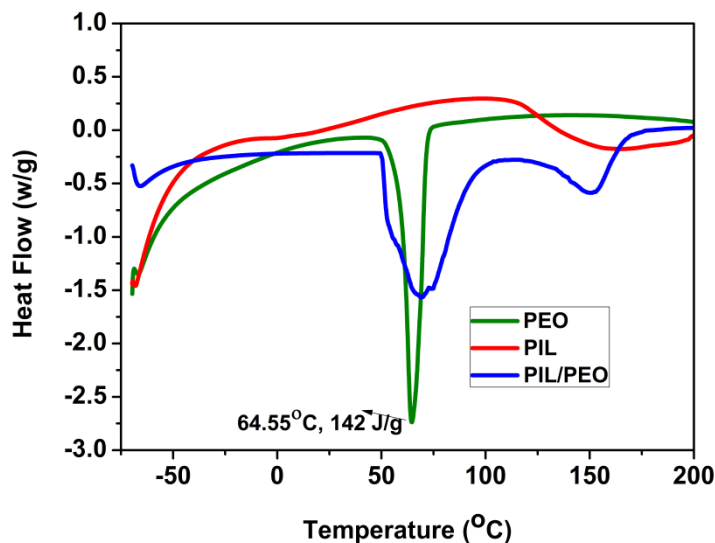


Figure 05. DSC thermogram of PEO nanofibers, PIL and PIL/PEO nanofibrous membrane

6.6. Electrolyte uptake (U), porosity (P) and Ionic Conductivity (σ)

The porosity (P) of the nanofibrous membrane was determined by immersing the electrospun membrane into n-butanol for 1 h. The weights of the nanofibrous membranes before (m_i) and after (m_a) immersion were measured. The densities of n-butanol and the sample were represented as ' ρ_b ' and ' ρ_s ' respectively. Porosity was evaluated by using the equation (2) (Mini & Sheeja, 2019).

$$P(\%) = \frac{\frac{m_a}{\rho_b}}{\frac{m_a}{\rho_b} + \frac{m_i}{\rho_s}} \times 100 \quad (2)$$

The equation (3) (Mini & Sheeja, 2019) was used to measure liquid electrolyte uptake in the electrospun membranes, where ' m_o ' and ' m ' are the weight of the nanofibrous membrane before and after imbibing the liquid electrolyte.

$$U = \frac{m - m_o}{m_o} \times 100 \quad (3)$$

The ionic conductivity (σ) of the membranes was obtained using equation (4) (Karuppanan et al., 2015).

Where, ' l ' is the thickness of the membrane, ' A ' is the area of the membrane and ' R ' is the bulk resistance of the electrolyte which was gained from the interception of an inclined straight line with the real axis in Nyquist plot.

$$\sigma = \frac{l(\text{cm})}{R(\Omega) \times A(\text{cm}^2)} \quad (4)$$

Ionic conductivity of PIL/PEO nanofibrous membrane based electrolyte was observed to have a higher value than that of the unblended PEO nanofibers. The reason could be due to the amorphous nature of the blend that could imbibe more liquid electrolyte into the pores. The charge carrier mobility enhanced due to an increase in amorphous nature. All the prepared polymer membranes exhibited good porosity due to their three dimensional network architecture (as shown in Table 01) that was appropriate for taking high amount of electrolyte which caused for the improvement in ionic conductivity.

Table 01. Physical analysis values of prepared membranes as electrolyte

Electrolyte	X _c (%)	U (%)	P (%)	σ (S cm ⁻¹)
PEO nanofibers	66	667	72	1.9x10 ⁻³
PIL/PEO nanofibers	31	903	89.8	3.7 x10 ⁻³

6.7. Photovoltaic Performances of DSSC

The electron transfer mechanism (Malaisamy et al., 2014) taking place in DSSCs containing PIL/PEO electrolyte are shown below:

N719 dye (D) absorbs photons and produces excited electron (D*)



The excited electron in the dye goes to the conduction band of TiO₂, to form the oxidized dye (D⁺), and the electron diffuses through TiO₂ coated anode and moves through the external load and reaches the Pt counter electrode.



The oxidized dye (D⁺) was regenerated by accepting electrons from reduced state I⁻ to produce the oxidized state I³⁻ of the electrolyte



Oxidized form of I³⁻ migrates to cathode through polymer electrolyte, and gets reduced to I⁻ by accepting electron from the Pt counter electrode (Pt CE).



Thus, DSSCs produce current from solar light without any chemical transformation. Iodine forms charge-transfer complex with the lone pair of electrons of nitrogen (N) atom in the imidazolium based PIL which prevents the recombination of triiodide present in the electrolyte and thereby inject electrons which increases the iodide concentration of the polymer electrolyte. Interconnected PIL/PEO electrospun nanofibrous membrane helps to entrap large amount of liquid electrolyte and thereby increase the stability of DSSCs.

Photovoltaic performance of the DSSCs were measured using LOT Technologies solar simulator equipped with a 150 W xenon under air mass 1.5 and 100 mW cm⁻² of light intensity.

Photovoltaic parameters, light-to-current conversion efficiency (η) and Fill Factor (FF) were calculated by using equation (5) and (6) as shown below (Khushboo et al., 2018).

$$\eta (\%) = \frac{V_{oc} J_{sc} FF}{P_{in}} \times 100 \quad (5)$$

$$FF = \frac{V_{max} J_{max}}{V_{oc} J_{sc}} \quad (6)$$

Where, 'J_{sc}' is the short-circuit current density, 'V_{oc}', the open circuit voltage and 'P_{in}' is the incident light power and J_{max} and V_{max} are the current density and voltage in the J-V curve at the point of maximum power on DSSC devices prepared using the electrospun nanofibers. The best results of V_{oc}, J_{sc}, FF, and η of the DSSC devices using the electrospun PIL/PEO nanofibrous membrane were found to be 0.65 V, 13.9 mA/cm², 0.59 % and 5.3 % under AM_{1.5}, respectively. J-V curves are shown in Figure 06. All the data of photovoltaic parameters of DSSCs under standard conditions are given in Table 02.

Table 02. Photovoltaic parameters of prepared membrane in DSSCs

Electrolyte	J_{sc} (mA/cm ²)	V_{oc} (V)	FF	η (%)
PEO nanofibers	11.76	0.43	0.52	2.62
PIL/PEO nanofibers	13.9	0.65	0.59	5.3

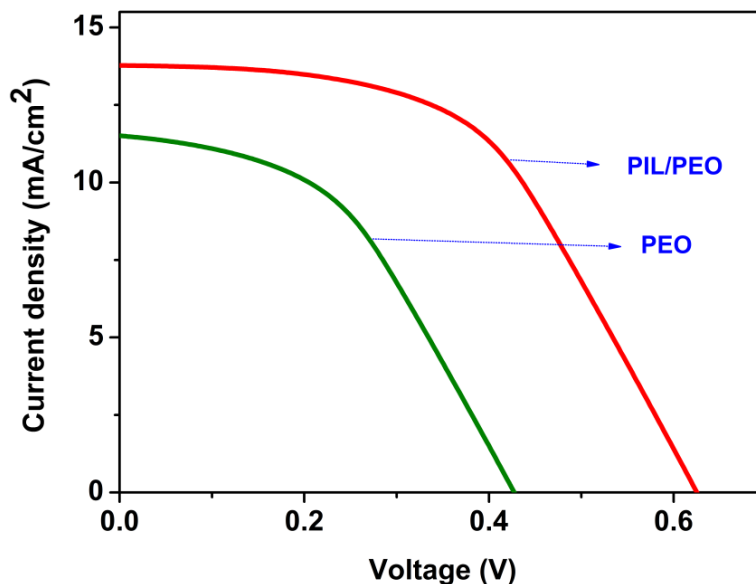


Figure 06. Photo current density-voltage (J - V) curves of prepared DSSCs with the PEO and PIL/PEO membrane as electrolyte

The overall power conversion efficiency of electrospun PEO was found to be lower than that of the PIL/PEO blend nanofibers as shown in Figure 06. This high efficiency value of PIL/PEO membrane was attributed to (1) the porosity of PIL/PEO blend that was higher than PEO (2) the fact that it can imbibe large amount of electrolyte (3) the good ionic conductivity (4) suppression of recombination reaction of electrons on the TiO₂ working electrode by the imidazolium part in the PIL (5) methyl methacrylate group in the PIL that helped to reduce the crystalline nature of PEO.

6.8. Stability measurement

In Figure 07 A, the stability of the QSS-DSSC using liquid electrolyte and PIL/PEO membrane was measured. In Figure 07 B, the total efficiencies were normalized to the values measured on the first day. The efficiency of the liquid cell decreased to 37% of their initial value after 5 days. The evaporation and leakage of organic solvent in liquid electrolyte caused the low stability of DSSC contained liquid electrolyte (Roger et al., 2014; Venkateswararao et al., 2014). Even if the power conversion efficiency of PIL/PEO membrane was initially 5.34%, it could be preserved up to 5.1% over the same test period of study. From the normalized power conversion efficiency graph it was clear that the efficiency of PIL/PEO membrane was maintained at 94% of their initial value after 5 days study period. It should be noted that PIL/PEO membrane exhibited better stability than liquid electrolyte cell because the polymer network prevented the leakage of electrolyte effectively.

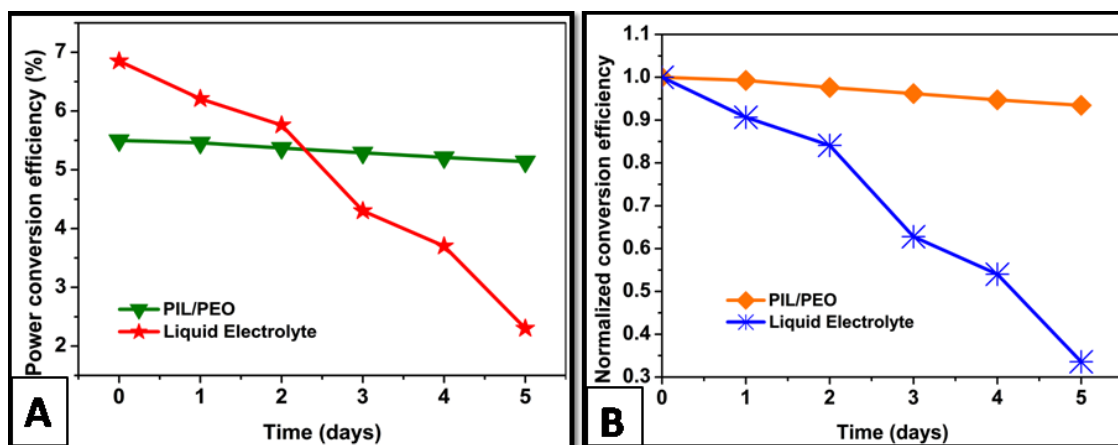


Figure 07. Stability measurement of DSSC with and without PIL/PEO membrane

7. Conclusion

The liquid electrolyte used in DSSC was found to be highly unstable. The present work is therefore aimed to increase the stability of the liquid electrolyte using a quasi-solid state electrolyte. To achieve this objective, poly (3-decyl-vinyl imidazolium methyl methacrylate tetrafluoroborate) (PIL) was synthesized, characterized and fabricated as electrospun membrane by blending with PEO and employed as an electrolyte for the fabrication of QSS-DSSC. The resultant PIL/PEO membrane based DSSC showed efficiency of 5.34% under the simulated solar spectrum illumination (100 mW cm^{-2}), which was higher than that of the PEO membrane based electrolyte. The electrospun nanofibrous membrane entrapped the liquid electrolyte in its three dimensional network structure, reduced leakage and evaporation of liquid electrolyte and thus enhanced the stability. The limitation of the prepared PIL/PEO membrane compared to liquid electrolyte was that it showed lower photo conversion efficiency due to low ionic conductivity. This is because the polymer matrix hindered the ionic mobility between electrodes. The prepared PIL/PEO membrane based electrolyte exhibited better stability (93.4% of its initial cell efficiency after 5 days) than the liquid electrolyte and thus showed good potential for future outdoor applications. The future work aims to increase ionic conductivity of the membrane and improve their conversion efficiency.

Acknowledgments

The authors gratefully acknowledge the instrumentation facility provided under FIST-DST and DRS-UGC to the Department of Chemistry, Anna University, Chennai. The instrumentation facility offered by the Department of Chemistry, IIT Madras is also gratefully acknowledged.

References

- Azli, A. A., Manan, N. S. A., & Kadir, M. F. Z. (2015). Conductivity and dielectric studies of lithium trifluoromethanesulfonate doped polyethylene oxide-graphene oxide blend based electrolytes. *Advances in Materials Science and Engineering*, <https://doi.org/10.1155/2015/145735>
- Buraidah, M. H., Shahan, S., Teo, L. P., Faisal, I. C., Careem, M. A., Albinsson, I., Mellander, B. E., & Arof, A. K. (2017). High efficient dye sensitized solar cells using phthaloylchitosan based gel polymer electrolytes. *Electrochimica Acta*, 245, 846–853. <https://doi.org/10.1016/j.electacta.2017.06.011>

- Chang, M., Erchuang, C., Junjing, L., Qingchao, F., Liqiang, W., Yan, S., & Jingli, S. (2018). Synthesis of mesoporous ribbon-shaped graphitic carbon nanofibers with superior performance as efficient supercapacitor electrodes. *Electrochimica Acta*, 292, 364-373. <https://doi.org/10.1016/j.electacta.2018.07.135>
- Deyab, M. A., Zaky, M. T., & Nessin, M. I. (2017). Inhibition of acid corrosion of carbon steel using for imidazolium tetrafluoroborate ionic liquids. *Journal of Molecular Liquids*, 229, 396-404. <https://doi.org/10.1016/j.molliq.2016.12.092>
- Elashmawi, I. S., & Gaabour, L. H. (2015). Raman, morphology and electrical behavior of nanocomposites based on PEO/PVDF with multi-walled carbon nanotubes. *Results in Physics*, 5, 105–110. <https://doi.org/10.1016/j.rinp.2015.04.005>
- Hao-Wei, P., Hsin-Fu, Y., Yi-June, H., Chun-Ting, L., & Kuo-Chuan, H. (2018). Electrospun membranes of imidazole-grafted PVDF-HFP polymeric ionic liquids for highly efficient quasi-solid-state dye-sensitized solar cells. *Journal of Materials Chemistry A*, 6, 14215-14223. <https://doi.org/10.1039/C8TA01215F>
- Ishanie, R. P., Akhil, G., Wanchun, X., Torben, D., Udo, B., Richard, A. E., Andre'Ohlina, C., & Leone, S. (2014). Introducing manganese complexes as redox mediators for dye-sensitized solar cells. *Physical Chemistry Chemical Physics*, 16, 12021-12028. <https://doi.org/10.1039/C3CP54894E>
- Karuppanan, P., Smita, M., & Sanjay, K. N. (2015). Chemically exfoliated nanosilicate platelet hybridized polymer electrolytes for solid state dye sensitized solar cells. *New Journal of Chemistry*, 39, 8602-8613. <https://doi.org/10.1039/C5NJ00795J>
- Khushboo, S., Vinay, S., & Sharma, S. S. (2018). Dye-sensitized solar cells: fundamentals and current Status. *Nanoscale Research Letters*, 13, 381-387. <https://doi.org/10.1186/s11671-018-2760-6>
- Luis, H., Sara, G., & Víctor, A. (2019). A review of photovoltaic systems: Design, operation and maintenance. *Solar Energy*, 188, 426-440. <https://doi.org/10.1016/j.solener.2019.06.017>
- Malaisamy, S., Subbiah, R., & Paramasivam, M. (2014). Preparation of PVDF-PAN-V₂O₅ hybrid composite membrane by electrospinning and fabrication of dye-sensitized solar cells. *International Journal of Electrochemical Science*, 9, 3166-3180.
- Marwa, F., Jehan, E. N., Mamoun, M., Shaker, E., Moataz, B. S., & Abd, El-Hady, B. K. (2016). Quasi-solid-state electrolyte for dye sensitized solar cells based on nanofiber PMA-PVDF and PMA-PVDF / PEG membranes. *International Journal of Electrochemical Science*, 11, 6064 – 6077. <https://doi.org/10.20964/2016.07.19>
- Mini, T., & Sheeja, R. (2019). Dye-sensitized solar cells based on an electrospun polymer nanocomposite membrane as electrolyte. *New Journal of Chemistry*, 43, 4444-4454. <https://doi.org/10.1039/C8NJ05505J>
- Muthuraaman, B., Viswanathan, E., Jiajia, G., & Lars, K. (2017). Polymer-doped molten salt mixtures as a new concept for electrolyte systems in dye-sensitized solar cells. *ACS Omega*, 2, 6570–6575. <https://doi.org/10.1021/acsomega.7b00925>
- Roger, J., Assaf, A., Piers, R. F. B., Li, X., Chunhung, L., & Brian, C. O. (2014). 2000 hours photostability testing of dye sensitised solar cells using a cobalt bipyridine electrolyte. *Journal of Materials Chemistry A*, 2, 4751-4757. <https://doi.org/10.1039/C4TA00402G>
- Shanmuganathan, V., I-Ping, L., Li-Tung, C., Yi-Chen, H., Chiao-Wei, L., & Yuh-Lang, L. (2016). Effects of TiO₂ and TiC nanofillers on the performance of dye sensitized solar cells based on the polymer gel electrolyte of a cobalt redox system. *ACS Applied Materials & Interfaces*, 8, 24559–24566. <https://doi.org/10.1021/acsmi.6b06429>
- Silvia, M., Gabriel, A., Ra'ul, P., Jairton, D., Mar'ia, I. B., Eduardo, G., & Santiago, V. L. J. (2017). Hierarchically structured polymeric ionic liquids and polyvinylpyrrolidone mat-fibers fabricated by electrospinning. *Journal of Materials Chemistry A*, 5, 9733–9744. <https://doi.org/10.1039/C7TA02447A>
- Tan, C. Y., Omar, F. S., Norshahirah, M., Saidi, F. N. K., Ramesh, S., & Ramesh, K. (2019). Optimization of poly(vinyl alcohol-co-ethylene)-based gel polymer electrolyte containing nickel phosphate nanoparticles for dye-sensitized solar cell application. *Solar Energy*, 178, 231–240. <https://doi.org/10.1016/j.solener.2018.12.043>

- Venkateswararao, A., Justin, T. K. R., Chuan-Pei, L., Chun-Ting, L., & Kuo-Chuan, H. (2014). Organic dyes containing carbazole as donor and π linker: optical, electrochemical, and photovoltaic properties. *ACS Applied Materials & Interfaces*, 6, 2528–2539. <https://doi.org/10.1021/am404948w>
- Xiaojian, C., Jie, Z., Jinyu, Z., Lihua, Q., Dan, X., Haigang, Z., Xiaoyuan, H., Baoquan, S., Gaohui, F., Ye, Z., & Feng, Y. J. (2012). Bis-imidazolium based poly (ionic liquid) electrolytes for quasi-solid-state dye-sensitized solar cells. *Journal of Materials Chemistry*, 22, 18018–18024. <https://doi.org/10.1039/C2JM33273F>
- Yanyan, D., Qunwei, T., Yuran, C., Zhiyuan, Z., Yang, L., Mengjin, H., Peizhi, Y., Benlin, H., & Liangmin, Y. (2015). Solid-state dye-sensitized solar cells from poly(ethylene oxide)/polyaniline electrolytes with catalytic and hole-transporting characteristics. *Journal of Materials Chemistry A*, 3, 5368–5374. <https://doi.org/10.1039/C4TA06393G>
- Yi-Feng, L., Chun-Ting, L., Chuan-Pei, L., Yow-An, L., Yamuna, E. R., Vittal, Ming-Chou, C., Jiang-Jen, L., & Kuo-Chuan, H. (2016). Multifunctional iodide-free polymeric ionic liquid for quasi-solid-state dye-sensitized solar cells with a high open-circuit voltage. *ACS Applied Materials & Interfaces*, 8, 15267–15278. <https://doi.org/10.1021/acsami.6b02767>
- Zebardastan, N., Ramesh, S., & Ramesh, K. (2017). Performance enhancement of poly (vinylidene fluoride-co-hexafluoro propylene)/polyethylene oxide based nanocomposite polymer electrolyte with ZnO nanofiller for dye-sensitized solar cell. *Organic Electronics*, 49, 292–299. <https://doi.org/10.1016/j.orgel.2017.06.062>